Femtosecond studies of the iodine–mesitylene charge-transfer complex

Stuart Pullen, Larry A. Walker II, and Roseanne J. Sension
Department of Chemistry, University of Michigan, Ann Arbor, Michigan 48109

(Received 27 April 1995; accepted 3 August 1995)

Femtosecond laser studies have been performed to investigate the initial photodissociation reactions of I_2–mesitylene charge transfer complexes. Photodissociation occurs along both the I_2–mesitylene ''bond'' and the I–I bond with a branching ratio of 2:3 for the two reaction coordinates. Following excitation at 400 nm, geminate recombination occurs along both reaction coordinates. The reformed I_2–mesitylene complexes are formed vibrationally hot and relax on a time scale of 13 ps. The I–mesitylene spectrum is fully developed within 500 fs of the pump pulse. Approximately 40% of the I–mesitylene complexes undergo geminate recombination on a time scale of 14 ps. Most of the remaining complexes recombine with their original partners on a time scale of 400 ps. The initial anisotropy of the photoproduct absorption is 0.09 ± 0.02. This low anisotropy is a direct result of the geometry of the complex and nature of the electronic transition rather than indicative of ultrafast motion toward an asymmetric transition state preceding dissociation.

I. INTRODUCTION

One of the outstanding problems in chemical physics remains a detailed understanding of chemical transformation in fluid environments. With the advent of femtosecond lasers it has become possible to address this problem directly by using real time spectroscopic techniques to study reaction dynamics in a wide variety of environments. In this paper we report on the use of ultrafast pump–probe transient absorption spectroscopy to study the photo-induced reactions in what should be a very simple system, the I_2–mesitylene electron donor–acceptor complex. There are several fairly basic reasons for choosing this system for investigation. The iodine charge transfer transition has been the subject of innumerable experimental and theoretical investigations since it was initially reported by Benesi and Hildebrand nearly 50 years ago.[1] Excitation of I_2 in aromatic solvents is known to produce aromatic–I atom complexes which are stable for microseconds, having lifetimes determined by the second order rate constant for recombination.[2] The absorption spectra of the I_2–aromatic complexes and their photoproducts are relatively well characterized. Excitation into the I_2–aromatic charge transfer band is also found to facilitate formation of the transition state for halogen addition to methylated aromatics.[2,3]

In addition to the plethora of steady state spectroscopic investigations, I_2 has also been much studied as a paradigm for elementary reaction dynamics in solution. A wide range of classic studies have been performed investigating the picosecond to nanosecond photo-induced predissociation, geminate recombination, vibrational, and electronic relaxation processes of I_2 in a wide range of solvent environments.[4–8] These experiments have inspired a multitude of theoretical studies.[4,9–11] Studies of I_2^- (Refs. 12–14) and I_3^- (Ref. 15) have also contributed to our understanding of elementary reaction dynamics and have inspired additional theoretical efforts.[16,17] The I_2–aromatic complexes should prove to be equally fruitful as a model for more complicated reactions in solution. While I_2 photodissociation is a one-dimensional problem, the photochemistry of I_2–aromatic complexes represents to first order a two or three dimensional problem. The primary reaction coordinates involve the I_2–aromatic stretching coordinate and the I–I bond. The bending coordinate may also be important. The internal coordinates of the aromatic may be neglected except as a bath for dissipation of excess energy in the complex.

Several picosecond and femtosecond studies of the I_2–mesitylene (I_2–MST) complex have been performed.[18–20] The early picosecond studies established the rapid formation of an I–MST complex but lacked the time resolution to elucidate the primary steps in the process. More recently, a femtosecond study was performed using 310 nm radiation to excite the charge transfer complex.[20] The results of this study were interpreted in terms of a very rapid reaction, branching between the I_2+MST and I+I–MST dissociation channels within 25 fs. Polarization anisotropy measurements were interpreted in terms of a severely distorted geometry for the I_2–MST transition state preceding dissociation.

The 310 nm excitation used in this earlier study lies on the high energy side of the I_2–MST charge transfer absorption band. In this current investigation the excitation wavelength is between 390 and 400 nm. Most of the data was obtained with 400 nm excitation, which lies on the red edge of the charge transfer absorption band (see Fig. 1). Excitation at 310 nm results in the deposition of an additional 7250 cm^{-1}/molecule when compared with 400 nm excitation. The effect of excitation energy on the observed excited state dynamics is dependent upon the form of the excited state potential energy surface and the ability of the complex to dissipate excess energy. It is reasonable to assume that excitation into the charge transfer band involves substantial displacement along both the I–I bond and the I_2–MST ''bond.'' Unless excess energy placed into these modes is rapidly dispersed by coupling with the MST bath, excitation at 400 nm should result in reaction dynamics that are substantially different from those observed following 310 nm excitation. It is even possible that excitation at 400 nm will produce a bound, predissociative excited state, while excita-

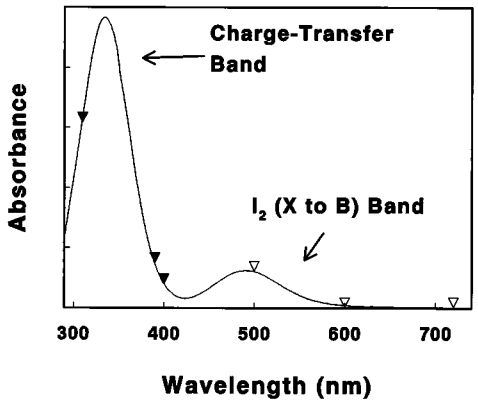

FIG. 1. The absorption spectrum of an iodine/mesitylene solution. The reference cell contained neat mesitylene. The peak at 334 nm is assigned to the charge-transfer absorption while the peak at 490 nm is an electronic transition of iodine. The filled triangles indicate the excitation wavelengths used in the current investigation and the excitation wavelength used by Lenderink *et al.* in Ref. 20. The open triangles indicate the probe wavelengths where the anisotropy of the photoproduct absorption was measured.

tion at 310 nm will be directly dissociative along both the I–I and I–MST coordinates. The results presented in this paper demonstrate that the reaction dynamics are indeed dependent upon the energy of the excitation pulse, although the complex is directly dissociative at both excitation wavelengths. Following 400 nm excitation, geminate recombination plays a dominant role in the recovery of ground state complexes. On the other hand, geminate recombination appears to play only a small role in the dynamics following excitation at 310 nm.[20] It is also shown that the initial low anisotropy of the photoproduct is a direct result of the geometry of the complex and nature of the electronic transition rather than indicative of ultrafast motion toward an asymmetric transition state.

II. EXPERIMENT

The kinetics and anisotropy of iodine in mesitylene solvent were recorded using a standard transient absorption pump–probe apparatus. A self-mode-locked titanium sapphire oscillator, running at 100 MHz and producing 20 fs, 2 nJ pulses, was regeneratively amplified following the standard scheme of Salin *et al.*[21] Following compression, the resulting laser beam is centered at 800 nm, with a bandwidth of approximately 25 nm, providing 300 μJ, 100–200 fs pulses at a repetition rate of 1 kHz. The pump and probe beams were produced by splitting the amplified Ti:sapphire output using a 50–50 beamsplitter. The probe pulses were delayed with respect to the pump pulses by a computer controlled motorized translation stage from Klinger (Newport). The pump pulses at 400 nm were generated by focusing the 800 nm beam into a 1 mm β-barium borate (BBO) crystal and collimating. A Schott glass BG-39 filter was used to remove the residual fundamental. This produced pump pulses with pulse energies of $\sim$40 μJ. Neutral density filters were used to further reduce the pump energy to $\sim$2 μJ/pulse. The signals were determined to vary linearly with pump energy between approximately 1 and 10 μJ/pulse.

A white light continuum was generated for use as a probe beam by focusing the other 800 nm beam into a 1 cm cell of flowing ethylene glycol. The desired wavelength was selected using a set of interference filters (IF) from Corion (full width at half maximum of 10 nm). A reference beam was obtained by $\sim$4% reflection off of a glass slide, while the remaining 96% was focused into the sample as the signal beam. Neutral density filters were placed after the IF filter to ensure that the probe beam was always much weaker than the pump beam and within a factor of 3 of the same intensity at all wavelengths. A probe wavelength of 400 nm was obtained by using a 300 μm potassium dihydrogen phosphate (KDP) crystal to generate the second harmonic of the laser beam. A BG-39 Schott glass filter and neutral density filters were used to remove the remaining fundamental and reduce the probe beam to the proper intensity. A one-color transient absorption experiment was also performed with 390 nm pump and probe wavelengths by tuning the laser system to 780 nm.

Data were recorded by using shot-to-shot normalization of the signal and reference beams. Basically the signal and reference beams were focused onto separate amplified diodes producing a current that was integrated in separate channels. The signal from each channel was digitized using a standard 12-bit analog-to-digital board in the same computer that controls the delay stage. The signal for each pulse was recorded as the base-10 logarithm of the ratio of the signal and reference channels, according to the Beer–Lambert equation. Data points for a single scan were generated by averaging the signals from 200 laser pulses. Several scans were taken at each wavelength to average out long-term fluctuations in the laser intensity.

For most of the experiments the pump and probe beams were polarized at the magic angle of 54.7° with respect to each other. The polarization of the probe beam was kept vertical with respect to the experimental setup by means of a polarizing cube following continuum generation. Separate cubes were used for the 400–700 nm and 600–1000 nm spectral regions. A waveplate in the pump beam permitted rotation of the polarization of the excitation pulse. Anisotropy data were recorded in the fashion described above, with the waveplate in the pump beam producing vertical or horizontal polarizations.

Samples of iodine (Aldrich 99.9%, as purchased) in mesitylene (Aldrich 99+%, as purchased) were prepared to give a solution of approximately 0.01 M iodine, resulting in an optical density of $\sim$0.8 at 400 nm for a 1 mm path length. The sample was kept in a reservoir at 11 °C and flowed through a quartz cell with a 1 mm path length. Ultraviolet–visible absorption spectra were recorded before and after each set of measurements was taken and a fresh sample was prepared each day to avoid sample degradation.

III. RESULTS

Transient absorption measurements were made of I_2 in mesitylene (MST) for twelve probe wavelengths ranging from 750 to 400 nm. These measurements are summarized in the surface plot shown in Fig. 2. At early times the raw signal exhibits an increase in absorption that is peaked

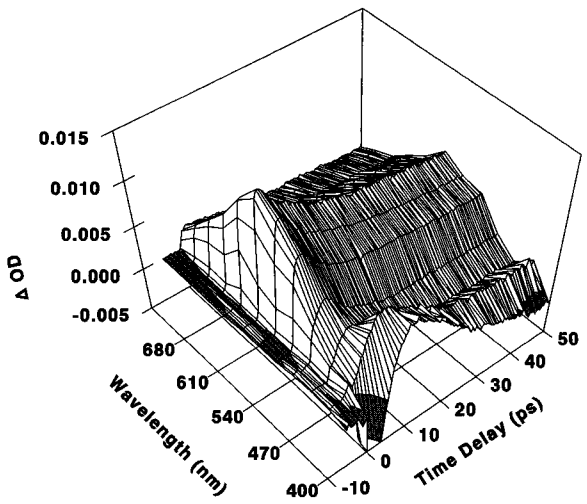

FIG. 2. Transient absorption signal obtained between 750 and 400 nm for a sample of iodine in mesitylene pumped at 400 nm.

around 600 nm. The spectrum observed at ~1 ps is shown in Fig. 3. At shorter wavelengths, where the I_2 $B \leftarrow X$ and I_2–MST charge transfer absorption bands occur, the signal contains a substantial contribution due to the bleaching of the ground state absorption. At no time is an absorption signal indicative of an ion pair $[MST^+, I_2^-]$ observed. I_2^- is characterized by a strong UV absorption band (~385 nm in polar solvents[22]) and a somewhat weaker near-IR absorption band peaking around 740 nm in both polar and nonpolar solvents.[14,23] MST^+ exhibits a visible absorption band at ~456 nm in the gas phase.[24] A ~35 nm red shift of this absorption in solution is expected, based on the observed shift for the hexamethylbenzene cation from 463 to 500 nm.[25] As will be seen below, the spectrum of the initial transient species may be consistent with the presence of a MST^+ absorption. However, neither of the I_2^- absorption bands are observed.

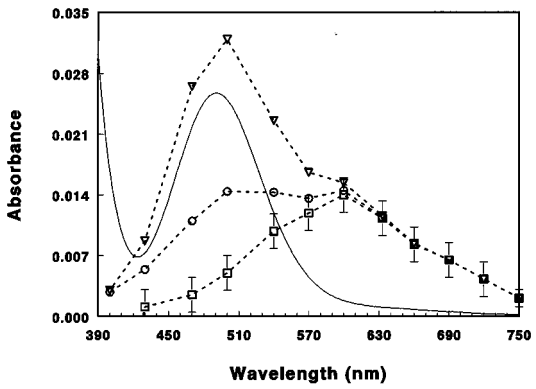

FIG. 3. Transient absorption spectrum 1 ps after excitation of the I_2–MST charge transfer band at 400 nm. The squares represent the raw data. This data has been corrected for the contribution of the I_2 bleach in two ways. (1) The circles represent the corrected spectrum assuming that only 35% of the complexes initially excited result in a bleaching of the I_2 local absorption. This is a lower limit on the magnitude of the bleaching contribution. (2) The triangles represent the corrected spectrum assuming that all of the complexes initially excited contribute to the bleaching of the I_2 local absorption. This is an upper limit on the magnitude of the bleaching contribution. The actual spectrum of the initial transient photoproduct lies between these two limits. The solid line is the spectrum of I_2 in mesitylene for reference.

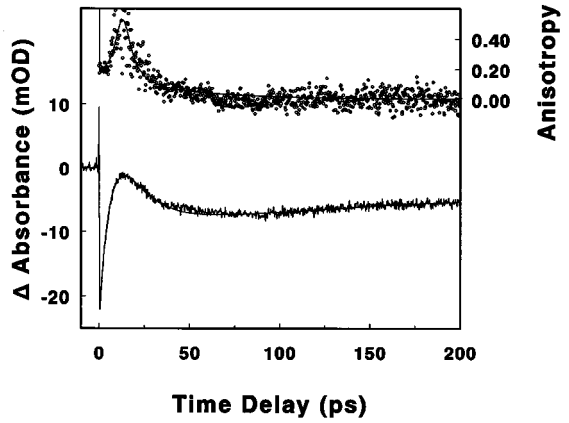

FIG. 4. Transient absorption signal (magic angle) and anisotropy obtained in a one-color pump–probe measurement of iodine in mesitylene at 390 nm. The data have been fit to a model consisting of bleaching signal with an initial anisotropy of 0.1 and a photoproduct absorption with an initial anisotropy of −0.2. The photoproduct absorption is 8 m o.d. at the earliest times and decays to 4 m o.d. with a time constant of 14 ps. There is a 65% recovery of the bleaching signal to a vibrationally hot ground state which appears in 7.3 ps and relaxes with a 12.5 ps time constant. The anisotropy of the bleaching signal decays on a time scale of 20–25 ps while the anisotropy of the photoproduct absorption decays on a time scale of 6 ps. This does not represent a unique fit to the data. See the text for an explanation of the significance of this model. The transient bleaching signal can be fit equally well using a model containing no photoproduct absorption. There is still a 65% recovery of the bleaching signal with a 7.3 ps appearance of the vibrationally hot complex and a 12.5 ps relaxation.

On the red edge of the transient absorption, $\lambda > 600$ nm, the observed signals consist of a biexponential decay of the transient absorption with decay components of 14 ± 2 ps and 350 ± 50 ps. The relative magnitudes of these two components vary with probe wavelength, indicating a slight narrowing or blue shifting of the transient spectrum with time. Data obtained in a one-color experiment at 390 nm demonstrates that the initial bleach of the charge transfer transition recovers substantially in a few tens of picoseconds. The data shown in Fig. 4 have been fit to a model consisting of a coherence artifact and an instrument limited bleach with a 7 ps recovery to a vibrationally hot complex. The hot complexes then cool on a time scale of 12–13 ps. The residual bleach has an amplitude ~35% of the initial bleach and recovers on a time scale of 400 ps (characteristic or $1/e$ time when fit to an exponential function).

The data obtained for $400 \leqslant \lambda_{probe} \leqslant 600$ nm contain competing contributions from photoproduct absorption and the bleaching of the ground state absorption. In order to analyze this data, the magnitude of the bleaching component must be estimated. The amplitude of the bleach observed at 400 nm and 390 nm indicates that at least 2.2% of the ground state complexes have been excited by the pump pulse. From the pump energy (~2 μJ) and spot size at the focus, it is estimated that 2.5% of the I_2–MST complexes have been excited. The discussion that follows will assume that the pump pulse places 2.5 ± 0.3% of the I_2–MST complexes present initially into the excited electronic state.

TABLE I. Equilibrium constants for the iodine–mesitylene complexation reaction.[a]

Sample type	Equilibrium constant	Temperature (°C)	Percent of iodine complexed	Reference
Iodine/MST in carbon tetrachloride				
1	0.43	25	0.76	26
2	0.58		0.81	27
3	0.82		0.86	28
4	0.72	22	0.84	1
Iodine/MST in heptane				
1	0.53	22	0.79	1
2	0.71	25	0.84	29
3	0.882	24	0.864	30
4	1.0454	14	0.883	30
Iodine/MST "free from solvent interaction"				
1	1.64	24	0.922	31

[a]Density of mesitylene (20 °C), 0.8652 g/mL; molecular weight of mesitylene, 120.2 g/mol; concentration of neat MST, 7.198 M.

The visible absorption band shown in Fig. 1 consists of contributions due to both complexed and uncomplexed I_2. Excitation at 400 nm or 390 nm should excite only complexed I_2. The equilibrium constant for the I_2–mesitylene complex has been measured on several occasions in both carbon tetrachloride and *n*-heptane solutions. These values are summarized in Table I, and are dependent upon both solvent and temperature. The percentage of I_2 complexed is calculated for each of the equilibrium constants reported in Table I. Based on these measurements we may safely assume that in our experiments 88%±4% of the available I_2 is complexed in the initial solution. The 400 nm pump pulse will therefore bleach 2.5% of 88% (or 2.2%) of the visible absorption band. This estimate provides an upper limit to the magnitude of the bleach.

One hypothesis regarding dynamics on the excited state potential is that excitation provides an ultrafast partitioning between two directly dissociative reaction pathways, one involving the breaking of the I_2–MST bond and one involving the breaking of the I–I bond.[20] In this case the initial bleach of the visible transition may be quite a bit smaller than that estimated above. Assuming that the dissociation correlates to ground state I_2, complexes which dissociate via the breaking of the I_2–MST bond will not bleach the visible transition. Thus a lower limit for the bleaching of the visible transition is obtained from the slow recovery component observed in the 390 nm data. At least 35% of the complexes initially excited produce I–MST fragments. Thus, at least $2.5\%\times35\%\times88\%=0.8\%$ of the visible transition is bleached.

Using the above estimates for the contributions of the ground state bleach to the observed signal, the "pure" transient absorption spectrum is estimated and plotted in Fig. 3 for both limits. From this estimate, the spectrum of the initial transient species (~1 ps) is seen to be very broad, spanning the entire visible spectrum. Note in particular the peak at 500 nm, in the region where a MST^+ absorption is expected. The magnitude of this peak is very sensitive to the estimate of the ground state bleach, but it seems clear that the data do not rule out the presence of a small MST^+ contribution at early times.

The concentration of I–MST complexes is too low for the 400 ps decay of the I–MST absorption to be attributed to second order diffusional recombination. If 2.5% of the I_2–MST complexes have been excited in a solution with an initial iodine concentration of 10^{-2} M, the concentration of residual I–MST complexes after the 14 ps geminate recombination is approximately $[\text{I–MST}]=(0.009\ \text{M})\times(0.025)\times(0.35)\times2=2\times10^{-4}$ M. The second order rate constant for the recombination of I–MST is $\sim10.4\times10^9$ L mol^{-1} s^{-1}.[2(c)] This will result in a halflife for I–MST of $(10.4\times10^9\ \text{M}^{-1}\ \text{s}^{-1}\times2\times10^{-4}\ \text{M})^{-1}=0.5\ \mu\text{s}$. Clearly the 400 ps decay of the I–MST signal and the I_2–MST bleaching signal is dominated by the recombination of pairs of I–MST complexes before diffusional escape. We did not obtain data for delay times longer than 200 ps, and thus cannot estimate the ultimate quantum yield for formation of the I–MST complex observed in microsecond experiments, except that it must be ~10% or less.

In addition to measurements of population kinetics with magic angle polarization, we have also made polarization anisotropy measurements at probe wavelengths of 390 nm, 500 nm, 600 nm, and 720 nm (see Figs. 4–6). The anisotropy is calculated from

$$r(t)=\frac{I_{\parallel}(t)-I_{\perp}(t)}{I_{\parallel}(t)+2I_{\perp}(t)}=\frac{I_{\parallel}(t)-I_{\perp}(t)}{I_{\text{TOT}}(t)}, \tag{1}$$

where $I_{\parallel}(t)$ and $I_{\perp}(t)$ are the transient absorption signals obtained with parallel and perpendicular pump–probe polarization geometries, respectively. For a signal from one species the anisotropy is directly related to the average angle between the pumped and probed transition dipoles, $\theta(t)$, by

$$r(t)=\tfrac{2}{5}\langle P_2[\cos\ \theta(t)]\rangle. \tag{2}$$

If more than one species contributes to the observed signal, as is clearly the case here, the calculated anisotropy is given by

$$r(t)=A_1(t)r_1(t)+A_2(t)r_2(t)+\cdots\ . \tag{3}$$

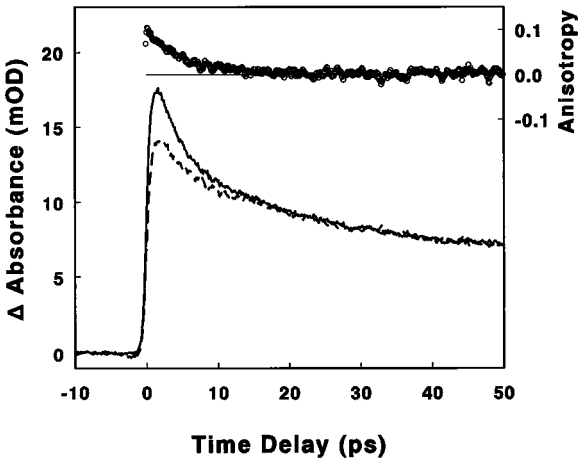

FIG. 5. Transient absorption signals for I_2 in mesitylene obtained with parallel (solid line) and perpendicular (dashed line) pump–probe polarization geometries. The pump and probe wavelengths are 400 and 600 nm, respectively. The resulting anisotropy is also plotted in the figure.

where $r_n(t)$ is related by Eq. (2) to the average angle between the pumped and probed transition dipoles for species n, $A_n(t)=I_n(t)/I_{\mathrm{TOT}}(t)$, and $I_n(t)$ is the total signal due to the nth component $[\Sigma_n I_n(t)=I_{\mathrm{TOT}}(t)]$. At 600 nm and 720 nm the signals are dominated by contributions from the photoproduct absorptions. These signals exhibit an initial anisotropy of $r(t=0)=r_0=0.09\pm0.02$ followed by an exponential decay of $\sim 8\pm 2$ ps. The decay of the anisotropy observed following excitation at 400 nm is much slower than that observed following excitation at 310 nm. An anisotropy measurement at 620 nm is reported in Ref. 20. These data also exhibited a low initial anisotropy of $\sim$0.10 which was followed by a biexponential decay with time constants of 320 fs and 1.5 ps.

The anisotropy of the bleach of the charge-transfer transition was made in a one color experiment at 390 nm. At this wavelength the anisotropy decay curve is complicated by the vibrational relaxation of the recovered complex and a coherence artifact when the pump and probe pulses are temporally overlapped. The coherence artifact has a high anisotropy of approximately 0.4. At longer times an anisotropy of 0.22 is observed which exhibits an overall decay of 25 ± 5 ps.

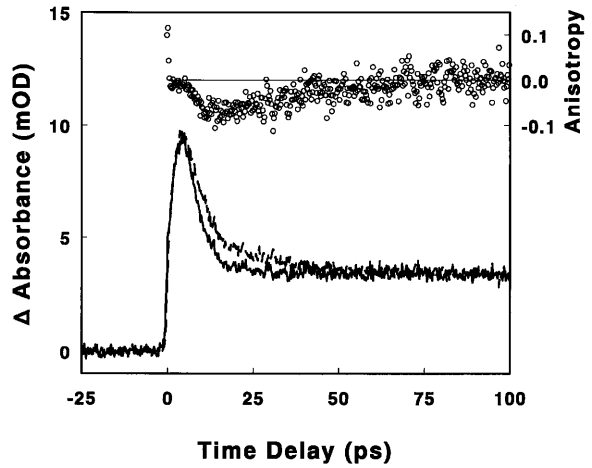

FIG. 6. Same as Fig. 5, except that the probe wavelength is 500 nm.

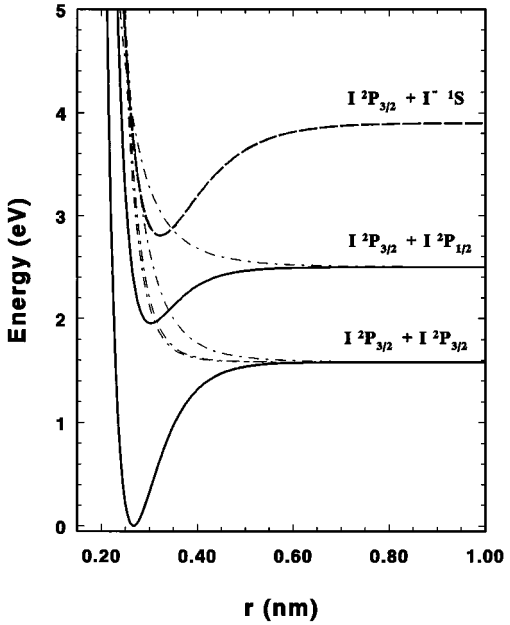

FIG. 7. Potential energy curves for I_2 and I_2^-. The solid lines are Morse oscillator potentials for the ground and excited B state of I_2 (parameters from Refs. 32 and 43). The dashed line is the potential for the ground state of I_2^- (parameters from Ref. 32). The energy of the I_2^- potential has been adjusted so that the vertical transition is at about 3.71 eV, consistent with the observed peak of the charge transfer absorption band. The dash–dotted lines are estimates for, from bottom to top, the $^3\Pi_g(2_g)$, $^3\Pi_g(1_g)$, $^3\Sigma_g^-(0_g^+)$, and $^3\Sigma_g^-(1_g)$ states of I_2 (Ref. 33). These states may influence the absorption spectrum or predissociation dynamics of the I_2^-–MST^+ complexes.

The signals measured at 500 nm contain contributions from both the ground state bleach and the photoproduct absorption, greatly complicating the interpretation. The data however, clearly indicate that the anisotropy of the bleach and the anisotropy of the photoproduct absorption are approximately the same. Because the signals are of comparable magnitude and opposite sign, the contributions roughly cancel.

IV. DISCUSSION

A. Initial dynamics

It is generally accepted that the UV transition of an iodine complex involves a transition from the ground electronic state of the complex to an excited state whose primary electronic configuration involves a donor/acceptor ion pair. The ground state potential energy surfaces of both I_2^- and MST^+ are bound. At first glance then, we would expect the charge-transfer state of the I_2–MST complex to be bound, with a potential surface resembling that of I_2^- along the I–I stretching direction, a potential resembling that of MST^+ along the MST coordinates and a Coulombic ion-pair potential along the I_2^-–MST^+ bond. In this case, application of the Franck–Condon principle to the excitation of I_2^- at 400 nm (3.10 eV) leads to the prediction of a bound complex, while 310 nm (4.00 eV) excitation is expected to lie above the I–I^- dissociation limit as shown in Fig. 7.[32]

Experimental data may be used to make a more accurate estimate of the vertical I_2^- potential in mesitylene. The vertical transition from MST–I_2 to MST^+–I_2^- peaks at 334 nm (3.71 eV). In work reported by Strong,[2] a broad absorption transition corresponding to I–MST and assigned to an I–MST to I^-–MST^+ charge-transfer transition is observed peaking at ~600 nm (2.07 eV). The dissociation limit of isolated I_2 is 1.58 eV.[32,33] This will be reduced slightly in the donor–acceptor complex, where the I_2 frequency is lower and the potential appears more anharmonic,[34] but it is certainly not less than 1 eV. Therefore the MST^+–I^-+I state is placed approximately 3.35 ± 0.3 eV above the ground state of the MST–I_2 complex. This dissociation limit also supports the prediction that excitation at 310 nm will lie above the dissociation limit, while excitation at 400 nm lies below the direct dissociation limit.

The transient absorption results obtained above do not support this simple picture however. The data show no evidence for a stable ion-pair state. There are at least two possible explanations for this. (1) The I–MST to I^-–MST^+ transition is highly displaced along the I–MST coordinate and the minimum for the I^-–MST^+ state lies at much lower energies. (2) The excited state may be predissociative, with internal conversion and dissociation occurring on a time scale fast compared to our temporal resolution of ~250 fs. These two possibilities are not mutually exclusive and may both play a role in the experimental observations.

The first possibility involves a reasonable assumption based on the observed absorption band for the I–MST transition, which is quite broad and structureless (see Ref. 2, Ref. 19, as well as the spectra reported here). In addition, the I–MST bond length is expected to be highly sensitive to the charge distribution. Therefore, the origin of the highly displaced I–MST→I^-–MST^+ transition undoubtedly lies below 1.77 eV (700 nm). Further support for this hypothesis comes from the calculation of Maslen *et al.*[17] These workers explored the effect of a static electric field on the I_2^- potential energy curves and came to the conclusion that such a field will have a large effect on the dissociation limit in the ground state. In the presence of a field of 0.006 a.u., the calculated I_2^- and $I+I^-$ states are approximately isoenergetic with a barrier to dissociation. From the above discussion it is apparent that the I_2^- potential in the I_2^-–MST^+ complex is highly perturbed by the presence of the MST^+ cation. As a result, the observation of a spectrum reminiscent of isolated ground state I_2^- is not expected, even if the excited state complex is weakly bound. A spectrum reminiscent of isolated MST^+ may be expected at the earliest times. However, the best self-consistent interpretation of the present results indicates that such an ion-pair state is very short lived.

The second possibility deals with the excited states of Iodine of *g* symmetry which are predicted to lie in the region of the charge-transfer absorption[33] (see Fig. 7). These states are all dissociative correlating with the $^2I_{1/2}+^2I_{3/2}$ or $^2I_{3/2}+^2I_{3/2}$ dissociation limits. Thus, even if the charge-transfer state is bound, it may be predissociative or mix with the locally excited I_2 states in such a manner as to be directly dissociative along the I–I bond. The charge-transfer state may also be predissociative along the I_2–MST bond.

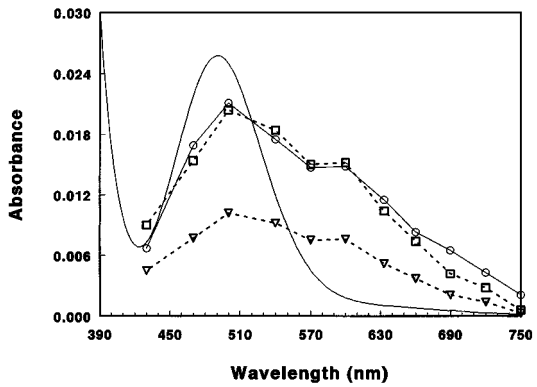

FIG. 8. Photoproduct absorption spectra 1 and 50 ps after excitation of the I_2–MST charge-transfer band at 400 nm. The circles represent the spectrum at 1 ps corrected for the bleaching of the visible transition of I_2 by assuming that 60% of the I_2–MST complexes initially excited dissociate along the I–I bond. The other 40% dissociate along the I_2–MST bond and do not contribute to the bleaching of the visible transition. The triangles represent the spectrum obtained at 50 ps corrected for the bleaching of the visible transition by assuming that 35% of the I_2–MST complexes initially excited form solvent separated I–MST complexes which recombine on a time scale of ~350 ps. Therefore 30% of the I_2–MST complexes initially excited are found as I–MST complexes at 50 ps. The squares represent the I–MST spectrum obtained at 50 ps multiplied by 2. Aside from a small amount of relaxation, I–MST complexes are formed within 300 fs. All further dynamics involve recombination of these complexes.

If the excited state potential energy surface is weakly bound, it is clearly predissociative with bond breaking occurring on a time scale of $\lesssim$250 fs. The model most consistent with the observed data involves direct dissociation along both the I–I and I_2–MST bonds. The signal which is attributed to absorption by the I–MST complex appears instantaneously within the resolution of the present experiments. The spectrum of this species changes very little with time thereafter as shown in Fig. 8. The branching ratio for I_2–MST to I–I dissociation is 2:3. At least 35% of the initially excited I_2–MST complexes form I–MST complexes. Because some of the complexes initially formed undergo geminate recombination, the yield for this channel will actually be somewhat higher. The ratio between the 1 ps and 50 ps spectra of the I–MST photoproduct indicates that 40% of the complexes initially formed undergo geminate recombination on a 14 ps time scale. Therefore 60% of the initially excited I_2–MST complexes dissociate along the I–I bond forming two I–MST complexes within 1 ps. There is a substantial geminate recombination in both of the dissociation channels.

B. Ground state relaxation

The data obtained between 570 nm and 390 nm contain a substantial component due to the vibrational relaxation of I_2–MST complexes produced either through ultrafast internal conversion to the ground state or, more likely, through geminate recombination resulting in the formation of vibrationally hot complexes. This is highlighted by the data obtained between 540 nm and 400 nm, which is plotted in Fig. 9, scaled in such a way as to emphasize the blue shift of the spectrum as a function of time (see also Fig. 2). The time constants are summarized in Table II. A small 1 ps rise is seen in the data obtained at 600 and 633 nm. This may be due to vibrational

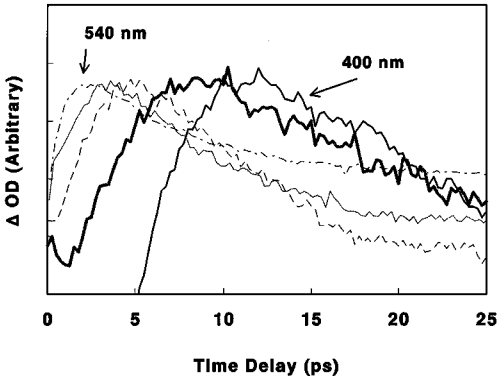

FIG. 9. Transient absorption kinetics for I_2–MST complexes excited at 400 nm and probed at 540 nm (dash–dotted line, labeled), 500 nm (light-solid line), 470 nm (dashed line), 430 nm (shaded line), and 400 nm (solid line, labeled). Note the time shift of the peak absorption intensity as a function of probe wavelength.

relaxation of the I–MST complexes or it may be attributed to the very earliest appearance of the hot I_2–MST ground state complexes. However, no rise is observed in the 660–750 nm spectral region. Thus, there does not appear to be an equivalent narrowing and red-shifting of the visible I_2 spectrum. This leads to the conclusion that geminate recombination produces an I_2–MST complex which contains little excess energy in the I–I bond. The vibrational relaxation is primarily along the I_2–MST bond, as is expected for fast cage recombination following dissociation along the reaction coordinate leading to I_2+MST. The portion of the signal observed at 570 nm that is attributed to vibrational relaxation of I_2–MST complexes rises on a time scale of 1.4 ± 0.3 ps. This sets a lower limit for the rate of ground state recovery, $k_{\text{recombination}} \geqslant 0.7\ \text{ps}^{-1}$.

For samples of I_2 in pure mesitylene, as were used in these experiments, the recombination could conceivably be either geminate recombination, where the iodine recombines with the same mesitylene molecule with which it was initially complexed, or random fast complexation with any of the mesitylene molecules in the immediate vicinity. Following excitation at 390–400 nm, it appears that the dominant mechanism for recomplexation involves geminate recombination. This conclusion is necessitated by the observation of the anisotropy at ~390 nm. The anisotropy of the bleach of the ground state complex starts at $\sim0.22\pm0.02$ and decays with a time constant of 25 ± 5 ps. At this probe wavelength

TABLE II. Time constants for the appearance and decay of signal due to vibrationally hot complexes.

Wavelength (nm)	τ (ps)	
	Rise	Decay
390	7.3	12.5
400	7.0	9.1
430	6.3	6.9
470	3.0	7.0
500	2.0	6.1
540	1.7	5.0
570	1.4	2.9

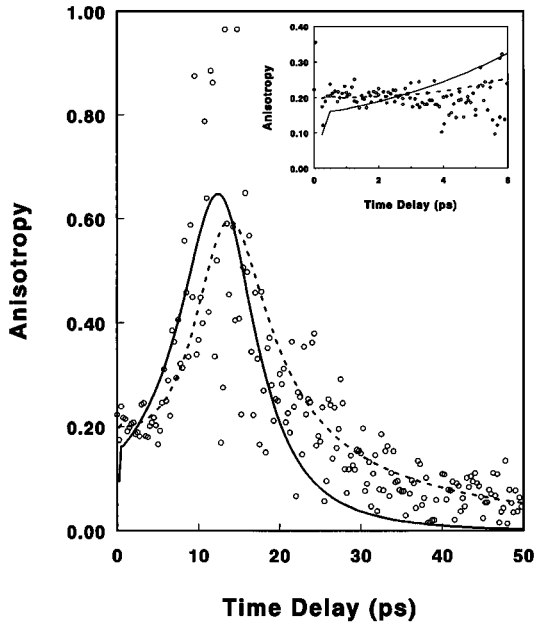

FIG. 10. The anisotropy in a one-color pump–probe experiment at 390 nm. The dashed line represents the calculated anisotropy assuming that the I_2–MST complexes that are reformed have essentially the same orientation as the I_2–MST complexes originally dissociated. For the bleach $r_0=0.2$ with a reorientation time of 25 ps. The initial anisotropy of the recovered absorption is 0.16 in this fit, consistent with a limited amount of random recomplexation. This slight randomization is required to account for the hump in the measured anisotropy near 12 ps. The solid line is the best fit obtained if the recovery of the bleach is assumed to be isotropic due to the random formation of complexes. Note that a random recomplexation is inconsistent with the flat anisotropy observed at early times and with the long overall decay time for the anisotropy.

the absorption of the vibrationally hot product appears with a time constant of 7.3 ± 0.3 ps and relaxes on a time scale of 12.5 ± 0.3 ps. If the recomplexation was random, the absorption due to the recovery of ground state I_2–MST complexes would be isotropic. As shown in Fig. 10, this is inconsistent with the observed data. The dominant mechanism for recomplexation following excitation around 390 or 400 nm is geminate recombination.

C. Anisotropy measurements

The anisotropy measurements presented above are capable, in principle, of providing a great deal of information on the reaction dynamics, the excited state symmetries, and the geometry of the ground and excited state complexes. The population kinetics and anisotropy signal obtained at 390 nm appears to be due primarily to the bleaching of the charge-transfer absorption and the subsequent partial repopulation of the ground state of the complex. In this case one would expect *a priori* to observe an initial anisotropy of 0.1 or 0.4 dependent upon the degeneracy of the excited state and the geometry of the complex.

In the point groups appropriate to the isolated molecules, the ground state of I_2^- has $^2\Sigma_u^+$ symmetry while the ground state of MST^+ is of E symmetry. The present consensus for the geometry of an I_2–aromatic complex appears to favor a symmetric axial arrangement of the I_2 over the plane of the

ring.[35–38] This arrangement has yet to be proven however.[39,40] An axial geometry is also proposed for the I–MST complex.[41] Data from femtosecond experiments on the I_2–hexamethylbenzene complex appear to indicate that the geometry of the complex is dependent on the solvent environment.[42] If the complex has an axial geometry and C_{3v} symmetry, the lowest energy ion pair state, $\psi[D^+,A^-]$, is doubly degenerate. The transition from the ground state of the complex (which is totally symmetric) to the excited state is polarized in the XY plane parallel to the plane of the aromatic molecule. Thus, if the complex is axial the initial anisotropy of the bleach should be 0.1. Because all in-plane transition moment directions are equally probable, the average angle between the pumped and probed transition moments is 45°.

The same reasoning holds for the I–MST complex. If the complex is axial, the lowest ion pair I^-–MST^+ state is doubly degenerate and the transition from I–MST to the I^-–MST^+ state should be polarized in the XY plane. Therefore, the initial anisotropy of the I–MST photoproduct signal is predicted to be 0.1, not 0.4 as assumed in Ref. 20. The observed initial anisotropy of absorption signals attributed to I–MST is 0.09 ± 0.02, in good agreement with the predicted value.

The initial anisotropy of the bleach measured at 390 nm, on the other hand, is observed to be $\sim$0.22, substantially higher than the predicted value of 0.1. There are two possible reasons for this apparent discrepancy. (1) The observed net bleaching signal at 390 nm contains contributions from the ground state bleach and a weaker photoproduct absorption. (2) The geometry is not axial, but rather, the iodine molecule is tilted with respect to the aromatic plane. Both of these possibilities will be discussed in greater detail below.

Transient absorption signals due to excited state absorption or photoproduct absorption bands are often observed in spectral regions where bleaching signals are expected. Care must always be taken to account for such contributions in the interpretation of the magnitude or anisotropy of a bleaching signal. In the present case the observed anisotropy may be accounted for if a z-polarized photoproduct transition contributes to the transient absorption signal at 390 nm. The transition moment of this z-polarized transition is perpendicular to the degenerate xy-polarized transition initially excited. Therefore, the initial anisotropy of this photoproduct absorption should be -0.2 corresponding to an average angle of 90° between the pumped and probed transition dipole directions. A bleach with an r_0 of 0.1 and an overlapping absorption with an r_0 of -0.2 will account for the observed anisotropy at 390 nm if the absorption is approximately 1/4 the strength of the bleach. This is the model used in the fit of the anisotropy shown in Fig. 4. The data are consistent with this model, although the fit is not unique and the present data are insufficient to prove this hypothesis.

The only reasonable assignment for such a photoproduct absorption is the transition from I–MST to the second I^-–MST^+ ion pair state. The first excited state of MST^+ is of A_2'' symmetry in the D_{3h} point group and correlates with A_1 in the C_{3v} point group of an axial complex. Therefore, the second ion-pair state is totally symmetric with respect to the overall symmetry of the complex, and the transition from the ground state will be z-polarized.

MST^+ exhibits a visible absorption band at $\sim$456 nm in the gas phase. A $\sim$35 nm red shift of this absorption in solution is expected, based on observed shift for the hexamethylbenzene cation.[25] Therefore this transition would be expected approximately 21 000 cm^{-1} above the transition to the first ion pair state, or around 37 000 cm^{-1} (270 nm) above the I–MST ground state. However, the state may be stabilized somewhat in the charge transfer complex. A highly displaced transition with a peak between 300 and 330 nm could contribute to the transient absorption signal at 390 nm. However, it seems unlikely that this transition could be sufficiently strong at 390 nm to account for the observed anisotropy.

The second option listed above probably accounts for the deviation of the observed anisotropy from the predicted value of 0.1. It is certainly possible that the instantaneous geometry of the I_2–MST complex is not axial. The experimental data and theoretical calculations are far from conclusive. A tilt of the I–I bond with respect to the symmetry axis of the mesitylene ring will break the degeneracy of the lowest I_2^-–MST^+ state. If the distortion and the electronic coupling are large, the two I_2^-–MST^+ states will separate substantially and the oscillator strength will be concentrated in one nondegenerate excited state having a unique transition dipole direction. In this case the initial anisotropy of the bleach will be 0.4. If the distortion is small the two states may remain nearly degenerate. However, the two electronic transitions will no longer have equal oscillator strengths and all in-plane transition directions will no longer be equally favorable. This will result in an initial anisotropy between 0.1 and 0.4. An anisotropy of 0.2 is consistent with a small distortion from an axial geometry and an average angle of 35° rather than 45° between the pumped and probed transition dipole directions. This is still consistent with an observed anisotropy of 0.1 for an axial I–MST photoproduct absorption. The average angle between the transition dipole moment for the pumped I_2–MST transition and probed I–MST transition will be $\sim$45° because all in-plane transition dipole directions are equally likely for the photoproduct absorption.

D. Comparison with excitation at 310 nm

There are several differences between the results reported in this paper for photodissociation of the I_2–MST complex at 390–400 nm and those reported by Wiersma and co-workers following excitation at 310 nm.[20] These are summarized as follows: (1) The signal that is observed at 500 nm following excitation at 310 nm shows little sign of the vibrational relaxation component that is prominent following excitation at 400 nm. The signal reported in Fig. 3 of Ref. 20 rises rapidly (apparently instrument limited) to its maximum, exhibits a plateau for $\sim$6–8 ps followed by a 13 ps decay to a residual absorption. (2) Following excitation at 310 nm, the photoproduct signal observed at 620 nm exhibits a 400 fs rise of a magnitude comparable to the instrument limited rise.[20] A small amplitude, $\sim$1 ps rise in absorption intensity

is observed at 600 and 633 nm following excitation at 400 nm. However, no rise is observed in the photoproduct absorption probed at 690 nm. (3) The anisotropy measured at 620 nm following excitation at 310 nm exhibits an initial value of 0.1 followed by a biexponential decay with components of 320 fs and 1.5 ps. This is in direct contrast to the data obtained at 600 and 720 nm following excitation at 400 nm, where the anisotropy decays with a single exponential time constant of $\sim 8 \pm 2$ ps from an initial value of 0.09 ± 0.02.

The low initial anisotropy was interpreted in the work of Lenderink *et al.*[20] in terms of ultrafast (<25 fs) motion towards the transition state. However, as discussed above, the value of $r_0 = 0.1$ is entirely consistent with the predicted polarization of the lowest I_2–MST and I–MST charge-transfer transitions. There is no need to invoke any kind of an ultrafast motion.

The fast biexponential decay of the anisotropy following excitation at 310 nm was interpreted in terms of rotational excitation due to the kick given to the I–MST fragment in the dissociation process. This may account for the 1.5 ps component. But there is a much more likely explanation for the 320 fs component, taking into account the observed 400 fs rise in the absorption signal at 620 nm. This rise was interpreted in terms of the formation of secondary I–MST complexes as in the scheme below,

$$I_2\text{–MST} \rightarrow I + \text{I–MST} \quad <25 \text{ fs}, \tag{Ia}$$

$$I + \text{MST} \rightarrow \text{I–MST} \quad 400 \text{ fs}, \tag{Ib}$$

where reaction (Ia) occurs directly upon excitation and reaction (Ib) accounts for the 400 fs rise. Presumably the I–MST complexes formed in reaction (Ib) in a three-dimensional solution of MST are largely random. That is, the orientation of the complex formed in reaction (Ib) is uncorrelated with the orientation of the original complex. This would immediately result in a ~400 fs decay of the anisotropy, consistent with the observation of a 320 fs decay. Approximately half of the observed signal arises from an isotropic distribution of I–MST complexes. The lack of a fast decay component in the anisotropy of the photoproduct following excitation at 400 nm is consistent with the lack of a rise in the transient absorption signal as well.

As there is a net production of I–MST complexes following excitation at 400 nm, reaction (Ib) must occur within 1 ps. Apparently the secondary complexes formed following excitation at 400 nm are not random. One possibility is that both I–MST fragments are formed directly upon excitation in complexes which have a sandwich geometry D–A—D. This would preserve the anisotropic polarization of the absorption transition for both I–MST fragments at early times. In a solution of I_2 in mesitylene an equilibrium between 1:1 and 2:1 or higher order complexes is expected. Excitation at 400 nm may selectively excite the 2:1 sandwich complexes relative to the 1:1 complexes. Alternatively, the residual kinetic energy of the I atom following excitation at 400 nm may be low enough that the atom is trapped by the nearest MST molecule, while excitation at 310 nm provides sufficient kinetic energy for the I atom to escape and complex randomly on a slightly longer time scale.

The differences observed in the kinetic signals at 500 nm and around 600 nm indicate that the reaction dynamics and/or the branching ratio for the two reaction pathways is modified by the excitation energy. Apparently the I_2–MST dissociation channel followed by geminate recombination and vibrational relaxation, which has a quantum yield of 0.4 following excitation at 400 nm, is relatively unimportant following excitation at 310 nm. If the complex undergoes dissociation to I_2+MST, the molecular iodine fragment interacts with the surrounding solvent before forming a randomly oriented complex with another MST molecule on a slower time scale. This randomization is a consequence of the somewhat higher kinetic energy of the fragments following excitation at 310 nm.

V. CONCLUSIONS

The most consistent model for the photodissociation reaction of I_2–MST complexes following excitation at 400 nm is as follows:

$$I_2\text{–MST} \rightarrow I_2 + \text{MST} \quad (\phi \approx 0.4), \tag{IIa}$$

$$\rightarrow 2\ \text{MST–I} \quad (\phi \approx 0.6). \tag{IIb}$$

This is followed by geminate recombination or escape,

$$I_2 + \text{MST} \rightarrow (I_2\text{–MST})^{\dagger} \rightarrow I_2\text{–MST} \quad (\phi \approx 1.0), \tag{IIc}$$

$$\text{MST–I} + \text{I–MST} \rightarrow I_2\text{–MST} + \text{MST} \quad (\phi \approx 0.4), \tag{IId}$$

$$\rightarrow \text{I–MST} + \text{MST–I} \quad (\phi \approx 0.6). \tag{IIe}$$

Geminate recombination of I_2 and MST in reaction (IIc) occurs on a time scale $\leqslant 1.4$ ps. Complete vibrational relaxation of the complex, $(I_2\text{–MST})^{\dagger} \rightarrow I_2$–MST, occurs on a time scale of ~13 ps. I–MST complexes either recombine according to reaction (IId) on a time scale of 14 ± 2 ps, or they escape or reorient to form solvent separated complexes. Most of these complexes also undergo geminate recombination on a time scale of ~400 ps. Those complexes which ultimately escape from each other recombine with a diffusion limited rate constant.[2]

The approximate quantum yield of 0.6 for the 14 ps escape process is determined from the decay of the photoproduct absorption signal at 600–660 nm. The transient absorption decays at longer wavelengths indicate larger apparent quantum yields for geminate recombination reaction (IId), but this is a result of concomitant narrowing of the I–MST spectrum due to a small amount of vibrational relaxation or solvation. The transient absorption spectrum corrected for the bleaching of the I_2 absorption band is shown in Fig. 8 for delay times of 1 and 50 ps. The contribution of the bleach at 50 ps is determined from the magnitude of the bleach recovery at 390 nm. The contribution of the bleach at 1 ps is estimated from a quantum yield of 0.60 for breaking the I–I bond. This is midway between the two limits in Fig. 4. The two spectra differ from each other by only a constant factor of 2, indicating that the 14 ps decay is a geminate recombination process.

The low anisotropy of 0.1 for the I–MST photoproduct absorption is accounted for by the fact that both excitation of the initial I_2–MST complex and the I–MST complex involve transitions to (nearly) degenerate states, polarized in the XY plane. There is no need to invoke a fast reorientation to form a transition state to account for the low anisotropy. It is a direct consequence of the symmetry of the complex.

As has been observed for I_2 excited into its visible transitions,[4] geminate or cage recombination plays a significant role in the reaction dynamics following photoexcitation of I_2–MST complexes. Approximately 65% of the initially excited complexes undergo cage recombination and account for the recovery of ground state complexes. Approximately 35% of the I–MST complexes escape from the cage or reorient to avoid fast recombination, but the majority of these ultimately recombine with their initial partners.

ACKNOWLEDGMENTS

Acknowledgment is made to the Donors of The Petroleum Research Fund, administered by the American Chemical Society, for partial support of this research. Further support was provided by the Center for Ultrafast Optical Science at the University of Michigan (NSF PHY-9319017) and the National Science Foundation (NSF CHE-9415772). We would also like to acknowledge the invaluable assistance of Dr. Jeff Squier and Dr. Steve Parus in the construction of our transient absorption system.

[1] H. A. Benesi and J. H. Hildebrand, J. Am. Chem. Soc. **71**, 2703 (1949).
[2] (a) S. J. Rand and R. L. Strong, J. Am. Chem. Soc. **82**, 5 (1960); (b) R. L. Strong, S. J. Rand, and J. A. Britt, *ibid*. **82**, 5053 (1960); (c) R. L. Strong, J. Phys. Chem. **66**, 2423 (1962).
[3] R. F. Cozzens, J. Phys. Chem. **79**, 18 (1975).
[4] A. L. Harris, J. K. Brown, and C. B. Harris, Annu. Rev. Phys. Chem. **39**, 341 (1988), and references therein.
[5] R. M. Bowman, M. Dantus, and A. H. Zewail, Chem. Phys. Lett. **161**, 297 (1989); M. Gutmann, D. M. Willberg, and A. H. Zewail, J. Chem. Phys. **97**, 8037, 8048 (1992); Ch. Lienau, J. C. Williamson, and A. H. Zewail, Chem. Phys. Lett. **213**, 289 (1993); Ch. Lienau and A. H. Zewail, *ibid*. **222**, 224 (1994).
[6] M. E. Paige and C. B. Harris, J. Chem. Phys. **93**, 3712 (1990); Chem. Phys. **149**, 37 (1990).
[7] R. Lingle, Jr., X. Xu, S.-C. Yu, H. Zhu, and J. B. Hopkins, J. Chem. Phys. **93**, 5667 (1990); X. Xu, S.-C. Yu, R. Lingle, Jr., H. Zhu, and J. B. Hopkins, *ibid*. **95**, 2445 (1991).
[8] R. Zadoyan, Z. Li, C. C. Martens, and V. A. Apkarian, J. Chem. Phys. **101**, 6648 (1994).
[9] D. E. Smith and C. B. Harris, J. Chem. Phys. **92**, 1312 (1990).
[10] H. Metiu and V. Engel, J. Chem. Phys. **93**, 5693 (1990).
[11] S. A. Adelman, R. Muralidhar, and R. H. Stote, J. Chem. Phys. **95**, 2738 (1991).
[12] J. M. Papanikolas, J. R. Gord, N. E. Levinger, D. Ray, V. Vorsa, and W. C. Lineberger, J. Phys. Chem. **95**, 8028 (1991); J. M. Papanikolas, V. Vorsa, M. E. Nadal, P. J. Campagnola, J. R. Gord, and W. C. Lineberger, J. Chem. Phys. **97**, 7002 (1992); J. M. Papanikolas, V. Vorsa, M. E. Nadal, P. J. Campagnola, H. K. Buchenau, and W. C. Lineberger, *ibid*. **99**, 8733 (1993).
[13] A. E. Johnson, N. E. Levinger, and P. F. Barbara, J. Phys. Chem. **96**, 7841 (1992); D. A. V. Kliner, J. C. Alfano, and P. F. Barbara, J. Chem. Phys. **98**, 5375 (1993); J. C. Alfano, Y. Kimura, P. K. Walhout, and P. F. Barbara, Chem. Phys. **175**, 147 (1993).
[14] J. C. King, M. C. Asplund, and C. B. Harris, in *Ultrafast Phenomena IX*, edited by P. F. Barbara, W. H. Knox, G. A. Mourou, and A. H. Zewail (Springer, Berlin, 1994), pp. 86–88.
[15] U. Banin, A. Waldman, and S. Ruhman, J. Chem. Phys. **96**, 2416 (1992); U. Banin, R. Kosloff, and S. Ruhman, Isr. J. Chem. **33**, 141 (1993); U. Banin and S. Ruhman, J. Chem. Phys. **99**, 9318 (1993); U. Banin, R. Kosloff, and S. Ruhman, Chem. Phys. **183**, 289 (1994).
[16] I. Benjamin, U. Banin, and S. Ruhman, J. Chem. Phys. **98**, 8337 (1993); I. Benjamin and R. M. Whitnell, Chem. Phys. Lett. **204**, 45 (1993); B. J. Gertner, K. Ando, R. Bianco, and J. T. Hynes, Chem. Phys. **183**, 309 (1994).
[17] P. E. Maslen, J. M. Papanikolas, J. Faeder, R. Parson, and S. V. ONeil, J. Chem. Phys. **101**, 5731 (1994).
[18] C. A. Langhoff, K. Gnädig, and K. B. Eisenthal, Chem. Phys. **46**, 117 (1980).
[19] E. F. Hilinski and P. M. Rentzepis, J. Am. Chem. Soc. **107**, 5907 (1985).
[20] E. Lenderink, K. Duppen, and D. A. Wiersma, Chem. Phys. Lett. **211**, 503 (1993).
[21] F. Salin, J. Squier, G. Mourou, and G. Vaillancourt, Opt. Lett. **16**, 251 (1991).
[22] P. Fournier de Violet, R. Bonneau, and J. Joussot-Dubien, Chem. Phys. Lett. **19**, 251 (1973).
[23] P. Fournier de Violet, R. Bonneau, and J. Joussot-Dubien, Chem. Phys. Lett. **28**, 569 (1974).
[24] H. H.-I. Teng and R. C. Dunbar, J. Chem. Phys. **68**, 3133 (1978).
[25] N. J. Peacock and G. B. Schuster, J. Am. Chem. Soc. **105**, 3632 (1983).
[26] J. A. Joens, J. Org. Chem. **54**, 1126 (1989).
[27] R. M. Keefer and L. J. Andrews, J. Am. Chem. Soc. **77**, 2164 (1955).
[28] L. J. Andrews and R. M. Keefer, J. Am. Chem. Soc. **74**, 4500 (1952).
[29] S. D. Christian, J. D. Childs, and E. H. Lane, J. Am. Chem. Soc. **94**, 6861 (1972).
[30] B. B. Bhomik and S. P. Chattopadhyay, Spectrochim. Acta **37A**, 135 (1981).
[31] B. B. Bhomik and S. P. Chattopadhyay, Spectrochim. Acta **37A**, 5 (1981).
[32] E. C. Chen and W. E. Wentworth, J. Phys. Chem. **89**, 4099 (1985).
[33] R. S. Mulliken, J. Chem. Phys. **55**, 288 (1971).
[34] W. Kiefer and H. J. Bernstein, J. Raman Spectrosc. **1**, 417 (1973).
[35] L. Fredin and B. Nelander, J. Am. Chem. Soc. **96**, 1673 (1974).
[36] H. Sakai, Y. Maeda, S. Ichiba, and H. Negita, J. Chem. Phys. **72**, 6192 (1980).
[37] S. Karaianev, E. D'Alessio, and H. Bonadeo, J. Am. Chem. Soc. **97**, 6474 (1975).
[38] I. Jano, Theor. Chim. Acta **66**, 341 (1985).
[39] A.-G. El-Kourashy and R. Grinter, J. Chem. Soc. Faraday Trans. II **1976**, 1860.
[40] E. Kochanski and J. Prissette, Nouveau J. de Chim. **4**, 509 (1980).
[41] A. Engdahl and B. Nelander, J. Chem. Phys. **78**, 6563 (1983).
[42] L. A. Walker II, S. Pullen, B. Donovan, and R. J. Sension, Chem. Phys. Lett. **242**, 177 (1995).
[43] D. J. Nesbitt and J. T. Hynes, J. Chem. Phys. **77**, 2130 (1982).